

Supplementary Information

**Spin-dynamics of the spin-correlated radical pair in Photosystem I.
Pulsed time-resolved EPR at high magnetic field**

O. G. Poluektov,* S. V. Paschenko, L. M. Utschig.

Chemical Sciences and Engineering Division, Argonne National Laboratory, 9700 S. Cass Ave.,
Argonne, IL 60439, USA

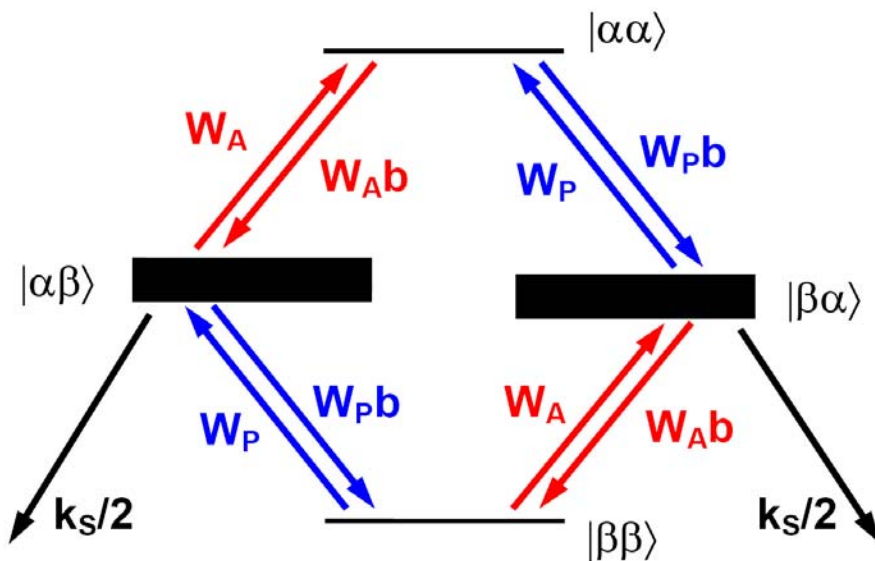
.

*To whom correspondence should be addressed. E-mail: Oleg@anl.gov

Theoretical approach

For the spectral simulation we followed the approach proposed in (S1-S3) with two minor modifications of the model. First, we define the eigenbasis of the Hamiltonian as $|\alpha\alpha\rangle$, $|\alpha\beta\rangle$, $|\beta\alpha\rangle$, $|\beta\beta\rangle$, where α , β denote the $1/2$, $-1/2$ projections of the individual unpaired electrons spins onto the magnetic field.^{S4,S5} This basis is more convenient for interpretation of the HF EPR spectra and treatment of the relaxation R operator than the triplet state basis T_+ , S, T_0 , T. used in^{S1}. Second, we include the possibility to treat the thermalization processes within radical pairs (RP) as described in the manuscript (scheme 1).

Scheme 1. Relaxation pathways within SCRPs



This is an absolute necessity because D-band spectra of spin correlated radical pairs recorded at long delay times exhibit Boltzmann population distribution. Importantly, for the limiting case, where $b = 1$, and $W_P + W_A = (T_1)^{-1}$, our approach is identical to the approach given in.^{S3} Thus, the population on the sublevel n_i can be described by:

$$n_i(t) = A_{i \text{ fast}} e^{-t/t_{\text{fast}}} + A_{i \text{ slow}} e^{-t/t_{\text{slow}}},$$

where decay times

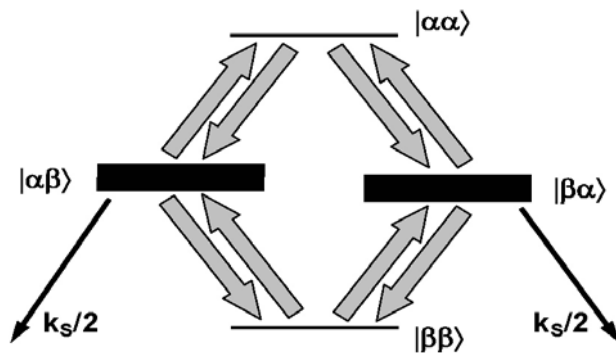
$$t_{\text{fast,slow}} = \left(k_S / 4 + 1/T_1 \pm 2\sqrt{(1/T_1)^2 + (k_S / 4)^2} \right)^{-1} \quad (*)$$

Let's consider specifically the two limiting cases of slow and fast relaxation:

1. Limiting cases: $T_1 \ll 4k_S^{-1}$

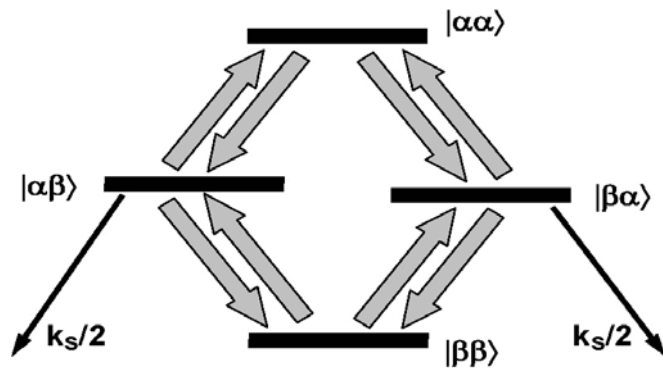
$$t_{\text{fast}} = T_1/2, \quad t_{\text{slow}} = 4k_S^{-1}$$

DAF ~ 0 :



Populations become equalized (or "Boltzmannized" for $b > 1$) fast

DAF $\gg T_1/2$:

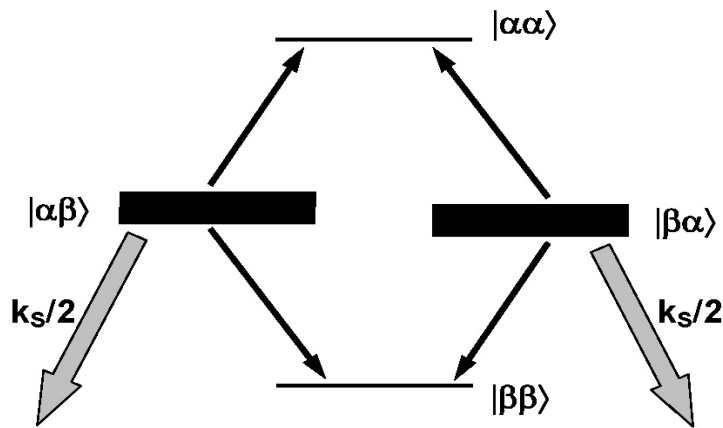


RPs can recombine only from two out of four levels, thus the effective decay time is $(1/4 k_S/2 + 1/4 k_S/2)^{-1} = 4k_S^{-1}$

2. Limiting case 2: $T_1 \gg 4k_S^{-1}$

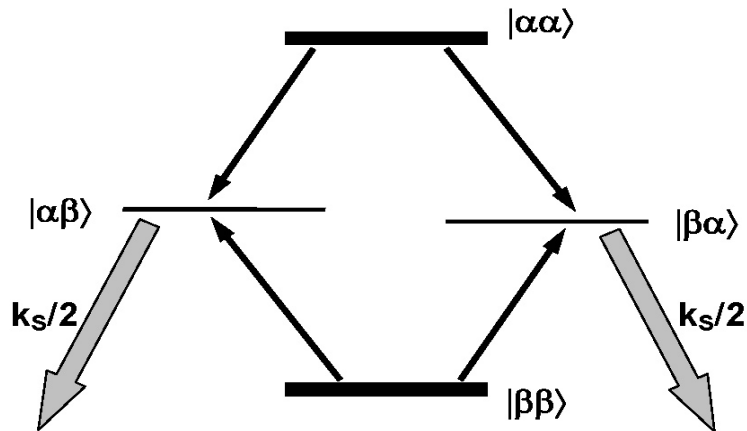
$$t_{\text{fast}} = T_1, t_{\text{slow}} = 2k_S^{-1}$$

DAF ~ 0 :



A majority of the RPs recombine from $|\alpha\beta\rangle, |\beta\alpha\rangle$. However, a small part of the RPs get into $|\alpha\alpha\rangle, |\beta\beta\rangle$ states before recombining

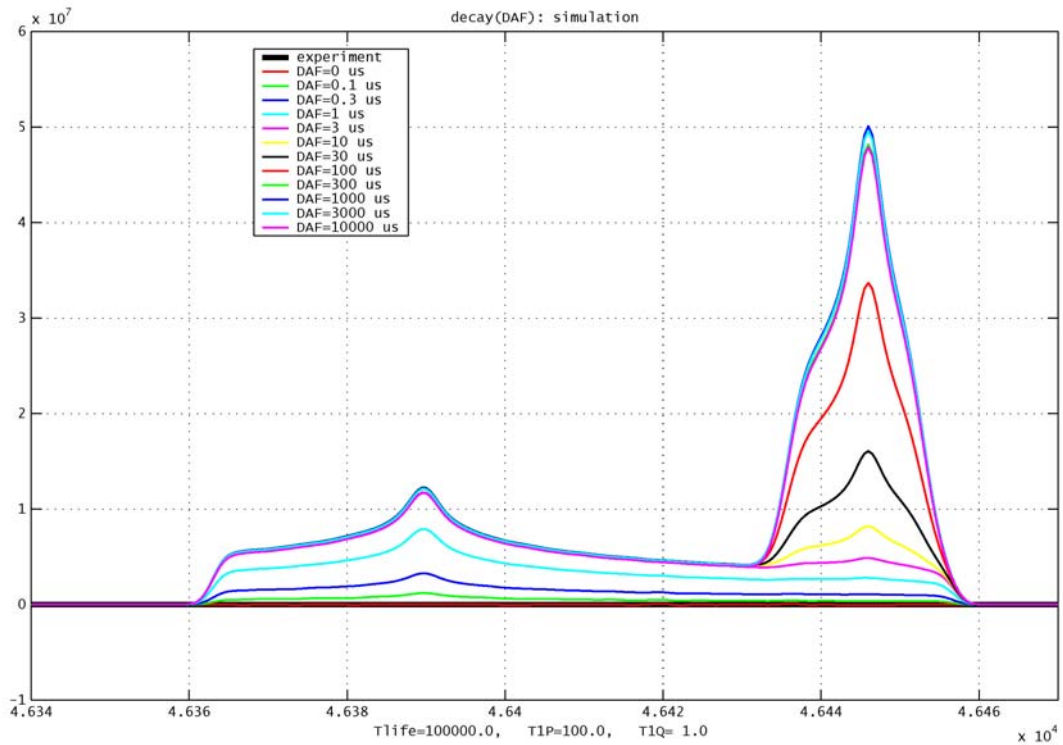
DAF $\gg 2k_S^{-1}$:



The lifetime of RPs in the $|\alpha\alpha\rangle, |\beta\beta\rangle$ states is T_1 . Populations are non-Boltzmann, and the resulting EPR spectrum resembles that at DAF=0, but is inverted. Our model allows one to calculate P^+Q^- RP decay with DAF for *unequal* values of the T_1 times of P^+ and Q^- .

To verify that our approach works in general and allows for simulation of the thermalized spectra even for different W_Q and W_P relaxation rates, let us consider the case of a very small interaction between the radicals ($D_{PQ}, J_{PQ} \rightarrow 0$).

For $W_P = (100 \mu\text{s})^{-1}$, $W_Q = (1 \mu\text{s})^{-1}$ (and for very small k_S), the model gives:

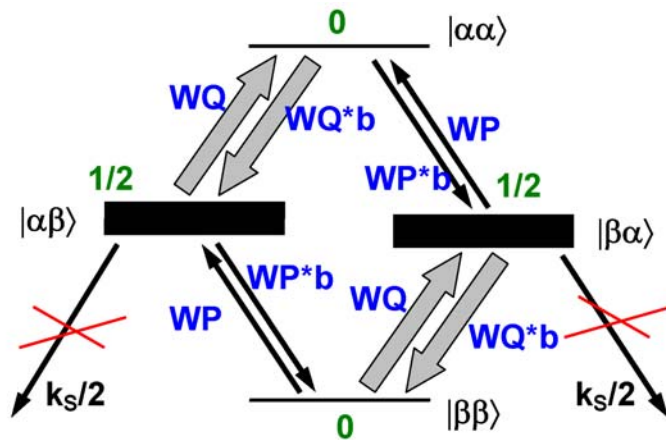


Student Version of MATLAB

RP spectrum = 0, as it should be for $D_{PQ}, J_{PQ} = 0$.

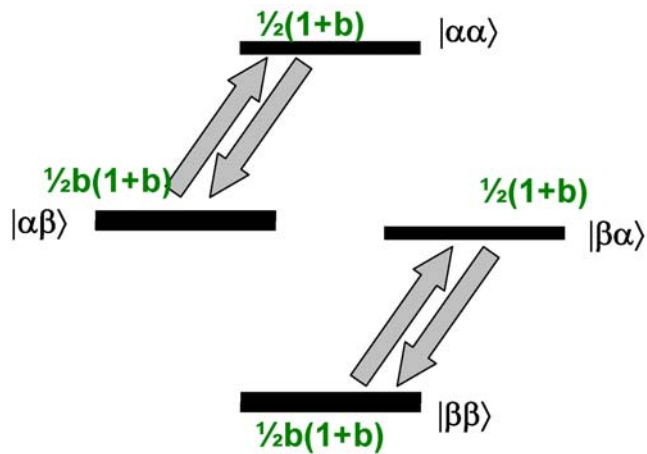
The Q-part of the RP spectrum becomes Boltzmannized with W_Q , P-part – with W_P .

This can be understood from qualitative considerations (they may seem trivial, but they might be useful for the case of non-zero coupling): let's look at any two levels for which one-quantum transition is possible. In equilibrium, the levels should be Boltzmann-populated: population of the lower level / population of the upper level = b , where $b \gg 1$ is the Boltzmann factor $\exp(\Delta E/kT)$. This condition means that "down" relaxation rate / "up" relaxation rate = b .

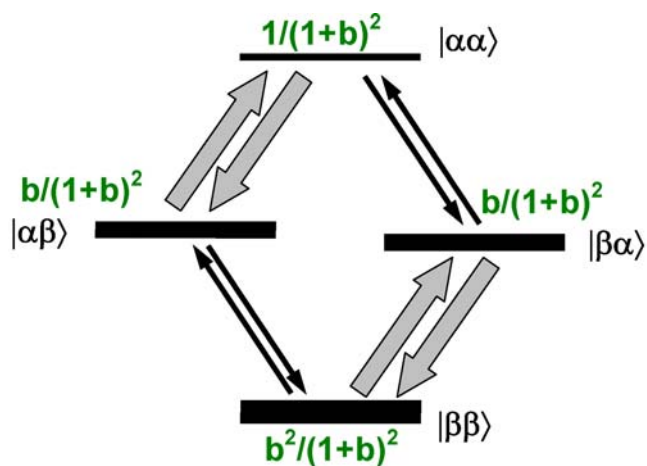


At DAF=0:

Populations (in green) of the ab , ba levels = $1/2$. (We assume that energy difference between ab and ba is much smaller than $\Delta E = h\nu$). Let's assume that $W_P \ll W_Q$. For this case, at $DAF \ll T_{1P}$, the system consists of two non-connected subsystems - pairs of levels (aa , ab) and (ba , bb). Boltzmannization in these pairs happens with time T_1Q , and ratio $\text{population}(ab)/\text{population}(aa) = b$ at all $DAFs \gg T_{1Q}$ (same for the other pair). At $DAF \gg T_{1Q}$ (but $\ll T_{1P}$), the populations are as follows:



Thus, for RP' the Q-part intensity is boltzmannized, while P-part $\rightarrow 0$ with WQ . At $DAFs \sim T_{1P}$, the relaxation between aa,ba and between ab,bb starts to occur. At very long $DAF \gg T_{1Q}, T_{1P}$, equilibrium is reached:



Here, population(lower level)/population(upper level) = b for every two levels (between which single-quantum transition exists). Both Q- and P-parts are boltzmannized. If b is close to 1, then the intensities of transitions $aa-ab$, etc. are the same as in the previous figure.

The simulations of SCRPs were done using the technique described in (S10)

The magnetic resonance parameters used for the simulation are presented in Table 1.

Table 1. Magnetic resonance and structure parameters used for EPR spectral simulations.

	g-tensor principal values ^d , (g_i-2)* 10^4 , where $i = X, Y, Z$			unresolved hfi tensor principal values ^a , mT		
	X	Y	Z	X	Y	Z
P^+	32.2	27.7	24.6	0.34	0.22	0.29
A_{1A}^-	63.6	52.0	23.1	0.25	0.25	0.25
	magnetic interactions		dipolar axis directions in			
	D, mT	J, μ T	P^+ g-tensor axes		A_{1A}^- g-tensor axes	
$P^+A_{1A}^-$	-0.17 ^c	5	φ^b	θ^b	φ^b	θ^b
			63°	39°	0°	79°

^a Unresolved hyperfine interactions (hfi) were simulated by a Gaussian lineshape with widths shown in the table.

^b φ and θ – azimuthal and tangential angles, respectively.

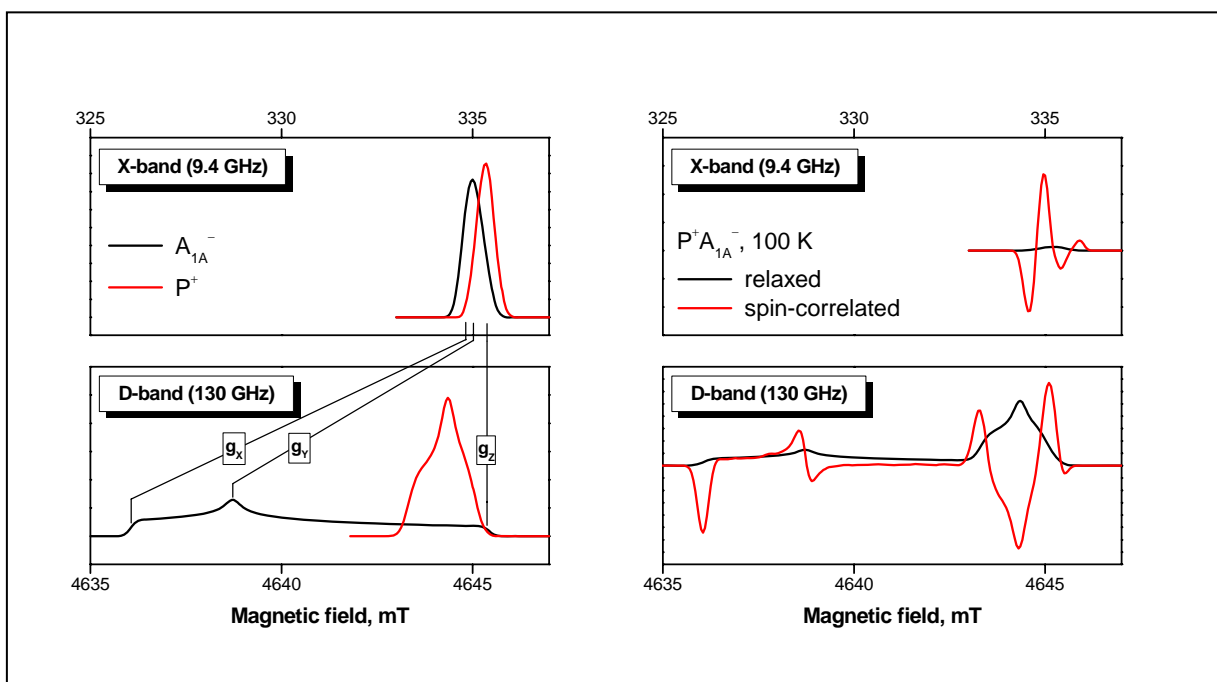
^c from^{S6-S8}

^d absolute values of g-tensor are calibrated according to^{S9}

Experimental.

The advantage of using HF EPR is demonstrated in Figure 1, where thermolized (left) as well as spin-correlated spectra of RP in PSI are shown. The left panel shows line shapes of the primary donor P^+ (black) and secondary acceptor A^- (red) at D-band and X-band EPR with a Boltzmann distribution of the sublevel populations. In the right panel the line shapes of SCRPs (red) is compared to the thermalized spectra (black). The ratio of intensities has been calculated for 100 K.

Figure 1. Comparison of the D-band and X-band EPR spectra of $P_{700}^+A_{1A}^-$ radical pair from the photosystem I reaction center protein.



Experimental time-resolved spectra of SCRPs in PSI were measured at D-band EPR and recorded at particular delays DAF-time minus a spectrum recorded before the laser flash. Figure 2 demonstrates some of these spectra recorded at different temperatures and DAF-times.

Decay kinetics were measured at D-band and X-band EPR by monitoring the spin-echo intensity as a function of the delay-time DAF. At D-band, EPR kinetic curves were measured at different magnetic field positions. All kinetics were fit with two exponential fitting routine. Some experimental curves and corresponding theoretical fit spectra are shown in Figure 3. Fit parameters are summarized in Table 2.

Figure 2. Deuterated PSI + 20 mM sodium dithionite (dark-adapted, dark-frozen)

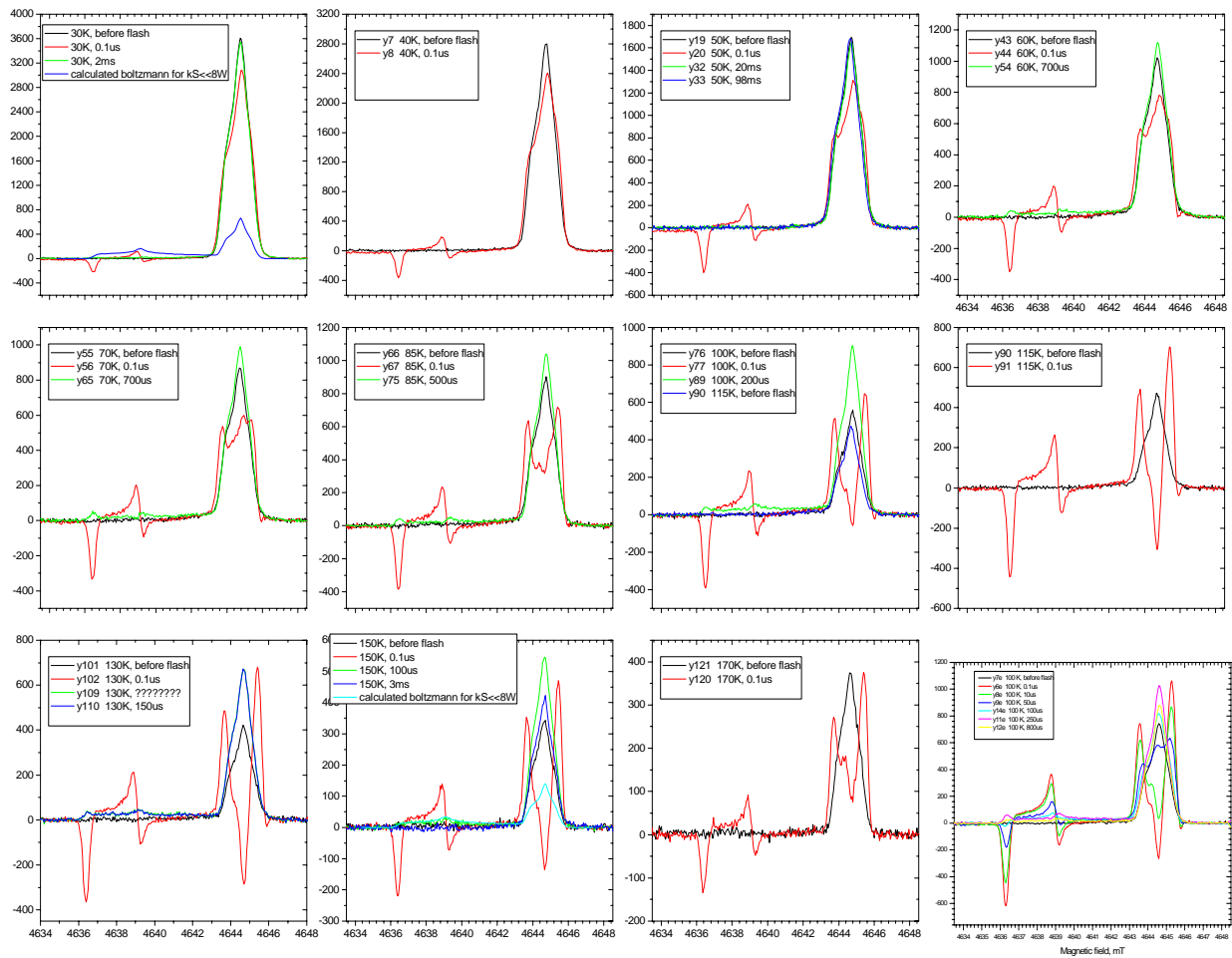


Figure 3. Typical DAF-kinetic D- and X-band EPR spectra recorded at different temperatures.

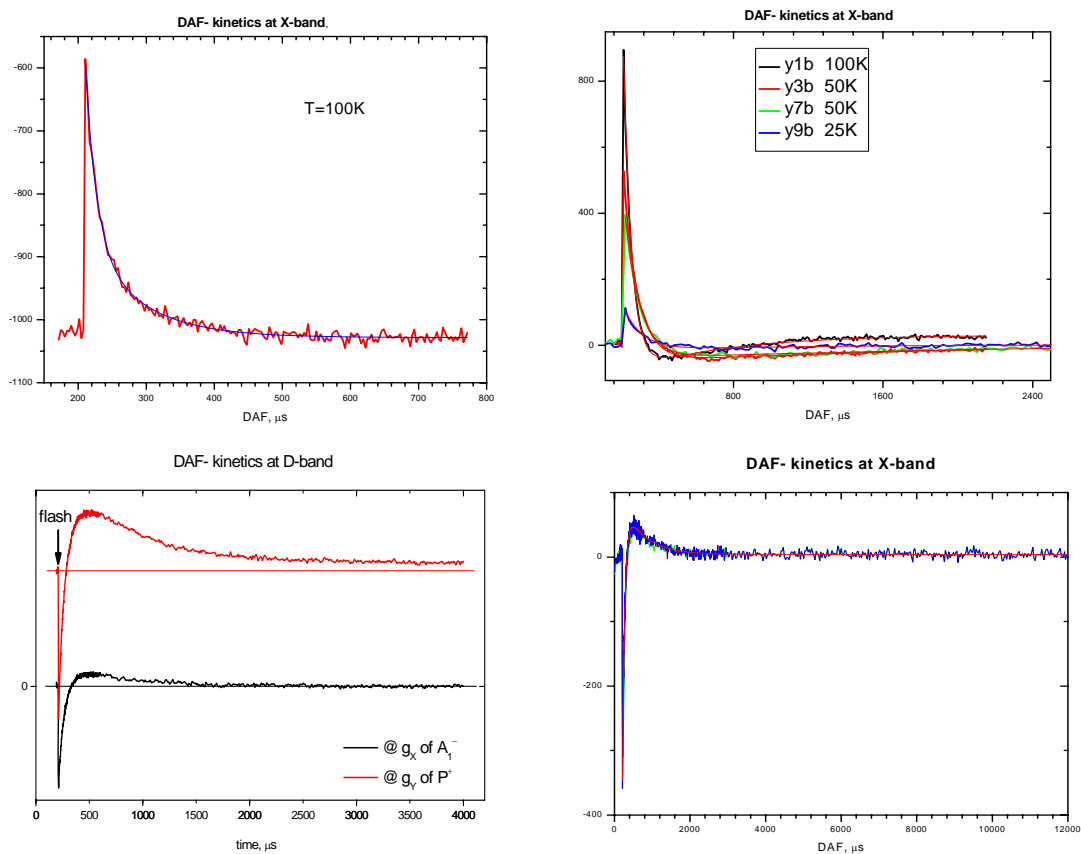


Table 2. Decay parameters obtained from bi-exponential fit of the experimental DAF-kinetics.

As measured at g_x component of Q^-

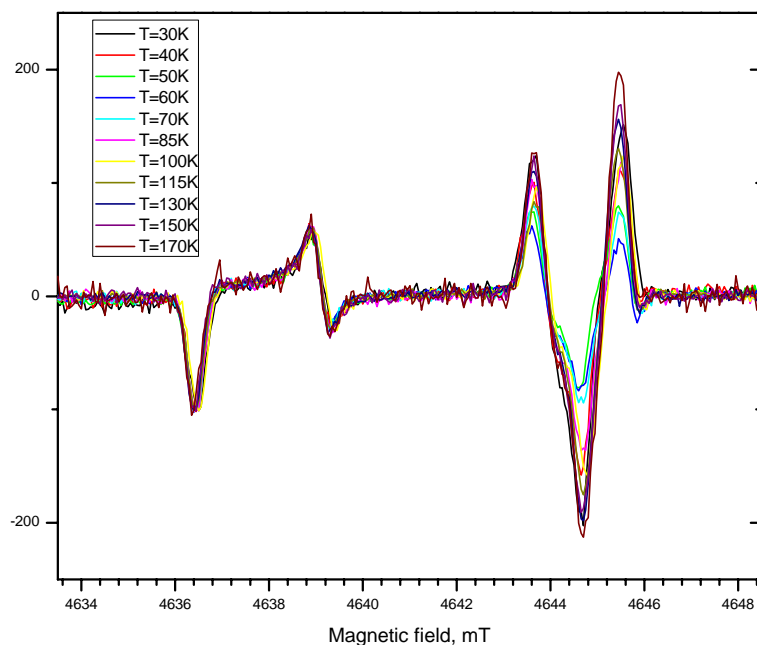
T	t_{fast}	t_{slow}	A_{fast}	A_{slow}
30	120.9	14200.9	-195.16318	15.2652
40	121.4	7382.9	-317.85724	34.59088
50	123.4	3493.9	-373.42303	49.45185
60	115.9	2004.4	-363.19096	54.03377
70	107.9	1369.0	-351.64225	59.15517
85	90.5	1013.2	-422.47604	76.59904
100	63.5	570.5	92.84152	73.51493
115	39.6	593.2	-463.90587	68.8602
130	25.1	510.9	-331.6714	40.54305
150	12.1	--	-205.85608	--
170	--	--	--	--

As measured at g_Y component of P^+

T	t_{fast}	t_{slow}	A_{fast}	A_{slow}
30	--	--	--	--
40	126.3	5925.7	-607.81253	209.20444
50	138.6	4402.9	-506.25317	192.87257
60	129.7	3104.7	-361.43389	124.7201
70	124.0	1965.6	-458.7723	144.8006
85	9.7	1171.7	-819.59202	290.4391
100	73.7	776.6	-676.21079	277.74674
115	48.8	574.1	-1157.273	404.8736
130	29.2	518.4	-982.76403	297.06896
150	15.6	436.0	-640.82114	165.34704
170	8.6	387.2	-296.09389	61.01018

It was observed that the relative intensities as well as the spectral lineshape of the P^+ and A^- part of the spectra of SCRP changes with temperature (see Figure 3). This effect has a maximum at temperature 60 K. We demonstrate that this temperature effect results from different T_2 times of the radicals within SCRP. This effect was not taken into account during the spectral simulation and was reduced by recording spectra with as short as possible τ -time.

Figure 3. Dependence of the radical pair lineshape on temperature.



REFERENCES.

- S1.** P. J. Hore, in: *Advanced EPR. Applications in Biology and Biochemistry*, ed. A. J. Hoff, Elsevier, Amsterdam 1989.
- S2.** U. Till and P. J. Hore, *Mol. Phys.*, 1997, **90**, 289.
- S3.** C. R. Timmel, C. E. Fursman, A. J. Hoff, P. J. Hore, *Chemical Physics*, 1998, **226**, 271.
- S4.** A. A. Dubinski, G. D. Perekhotsev, O. G. Poluektov, T. Rajh and M. C. Thurnauer, *J. Phys. Chem. B*, 2002, **106**, 938.
- S5.** O. G. Poluektov, L. M. Utschig, A. A. Dubinskij, and M. C. Thurnauer, *J. Am. Chem. Soc.*, 2005, **127**, 4049.
- S6.** R. Bittl, S. G. Zech, *J. Phys. Chem. B*, 1997, **101**, 1429.
- S7.** S. A. Dzuba, H. Hara, A. Kawamori, M. Iwaki, S. Itoh and Y. D. Tsvetkov, *Chem. Phys. Lett.*, 1997, **264**, 238.
- S8.** S. Santabarbara, I. Kuprov, W. V. Fairclough, S. Purton, P. J. Hore, P. Heathcote and M. C. W. Evans, *Biochem.*, 2005, **44**, 2119.
- S9.** O. G. Poluektov, L. M. Utschig, S. L. Schlesselman, K. V. Lakshmi, G. W. Brudvig, G. Kothe and M. C. Thurnauer, *J. Phys. Chem. B*, 2002, **106**, 8911.
- S10.** O. G. Poluektov, S. V. Paschenko, L. M. Utschig, K. V. Lakshmi, and M. C. Thurnauer, *J. Am. Chem. Soc.*, 2005, **127**, 11910.